Eurasian Chem.-Technol. J. 27 (2025) 229–234
The journal of the Institute of Combustion Problems https://ect-journal.kz

https://doi.org/10.18321/ectj1670

Luminescent Properties of a Solid-Phase Composite Based on Zirconium, Rare Earth Elements (Er, Nd) and Molybdenum

Lusik Nersisyan*, Romik Harutyunyan, Armen Martiryan, Hayk Petrosyan

Yerevan State University, 1 A. Manoogian Str., 0025 Yerevan, Armenia

Article info

Received:
29 March 2025

Received in revised form:
12 May 2025

Accepted:
23 June 2025

Keywords:
Luminescent
Rare-earth elements (REE)
Heterogeneous nanomaterials
Emission
X-ray

Abstract

As a result of the chemical synthesis, a heterogeneous compound with luminescent properties was obtained, containing rare-earth metal ions (Er^{3+}, Nd^{3+}), Mo^{6+}, and Zr^{4+}. The reaction was carried out using solutions of Na_2MoO_4, $ZrOCl_2$, $NdCl_3$, and $ErCl_3$ at a temperature of 22 °C. After 30–35 days, the system reached equilibrium, and an insoluble greyish-blue precipitate was formed. ICP-AES analysis confirmed the presence of all the initial components and showed the heterogeneity of the material; the molar ratio nNa : nMo : nZr : nEr : nNd = 0.05 : 0.22 : 0.086 : 0.082 : 0.05 was confirmed in the system. X-ray microanalysis revealed a complex multiphase structure characterized by significant chemical diversity and the presence of nanoparticles. Partial emission of Nd^{3+} at a wavelength of around 885 nm ($^4F_{3/2} \rightarrow {}^4I_{9/2}$ transition) was found by luminescence investigations; this can be utilised in medical near-infrared laser systems. Spectrometer constraints prevented the detection of Er^{3+} emission. The material's molybdenum-based structure and the presence of Zr^{4+} ions are responsible for the visible glow. Although more research is necessary to completely comprehend the Er^{3+} emission, the acquired findings suggest the possibility of developing complex heterogeneous luminous compounds containing rare earth ions for optical and medicinal applications.

1. Introduction

The prospects for using functional materials containing Zr^{4+}, REE, $[MoO_4]^{2-}$ in the chemical and optical industries, as well as in medicine, nuclear and semiconductor technologies, and in laser, magnetic, and phosphor applications, arise from the diversity of their properties [1–3]. Molybdates containing rare-earth element (REE) ions are of particular scientific interest due to their potential as phosphors with high color-rendering efficiency. In recent years, REE compounds, including REE molybdates, have been widely used in the production of X-ray phosphors [4–6].

In REE luminophores, the activators are REE ions, and the efficiency of emitters of this type appears when the activator ions are in inorganic systems, which are isostructural, solid powder phases. Their powder form allows for a significant expansion and simplification of practical application [7, 8].

REE molybdates, which contain two REE cations, are effective luminescent materials that emit red light under the influence of ultraviolet rays even in low concentrations, providing high brightness [9].

Zirconium compounds have different physical and chemical properties depending on their form and environment [10]. For example, zirconium dioxide (ZrO_2) is a refractory oxide that is used in thermal barrier coatings, dental ceramics, and solid oxide fuel cells [11, 12]. Zirconium molybdate is of particular interest because some of its forms exhibit negative expansion upon heating, it combines well with ceramics, and can be used in thermal management applications. In addition, zirconium-based compounds can form stable structures with molybdate anions, allowing the development of materials with tailored optical, catalytic, and structural properties [13, 14].

Another interesting aspect is compounds containing zirconium and lanthanides, such as Ln^{3+}-enriched ZrO_2 or zirconium and lanthanide-containing molybdates. Trivalent lanthanide ions (Ln^{3+}) doped with zirconium dioxide (ZrO_2) exhibit improved structural

*Corresponding author.
E-mail address: nersisyanlusik@mail.ru

stability and functional properties [15]. The introduction of lanthanides improves ionic conductivity and thermal stability by stabilizing high-temperature tetragonal or cubic phases and creating oxygen vacancies [16, 17]. Such compounds are more resistant to heat and permeation changes, have good ion permeability, and in some cases, light-emitting and radiation-resistant properties. This expands the possibilities of their application in functional ceramics and modern composite materials [18].

Neodymium (Nd^{3+}) has unique luminescent properties, which is why it has found application in various high-tech areas. Here are the main areas of its use:

1. Laser technology – neodymium lasers (Nd:YAG, Nd:YVO4, Nd:glass),
2. Medicine – used in surgery (tissue coagulation, tumor removal), ophthalmology (vision correction), dermatology (tattoo removal),
3. Industry – cutting, welding and engraving of metals, ceramics,
4. Military equipment – laser rangefinders and target designators,
5. Scientific research – as sources of monochromatic radiation,
6. Optical materials – glasses and crystals with Nd^{3+}, amplifiers of optical signals in telecommunications (fiber optics),
7. Filters and sensors – operating in the IR range,
8. Phosphors and backlighting LED technology – neodymium is added to phosphors to improve the color rendering of LEDs,
9. Screens and displays – in some types of plasma panels and specialized displays [19–23].

The aim of the work is to synthesize an inorganic compound containing rare earth ions $[MoO_4]^{2-}$ and zirconium. The relevance of the research is due to the critical role of rare earth and zirconium compounds in radio electronics, instrument-making and mechanical engineering, as well as the widespread use of their molybdates in medicine, various industries and advanced technologies [24].

In this work, Er^{3+} and Nd^{3+} ions were chosen as activators as various types of luminescent activators, allowing one to obtain a large number of luminophores of the same structural type.

2. Experimental part

The following compounds were used as starting compounds: $Na_2MoO_4 \cdot 2H_2O$ (≥99.5%, Merck, Germany), $ZrOCl_2 \cdot 8H_2O$ (98%, Merck, Germany), $ErCl_3 \cdot 6H_2O$ (99.995%, Merck, Germany), $NdCl_3 \cdot H_2O$ (≥99.99%, Sigma Aldrich, USA). Preparation for the study of the chemical reaction between $ZrOCl_2$, $ErCl_3$, $NdCl_3$ and Na_2MoO_4 in an aqueous medium was carried out at a temperature of 22 °C as follows: a solution of Na_2MoO_4 was poured into a 25 ml beaker, to which solutions of $ZrOCl_2$, $ErCl_3$, $NdCl_3$ were added in such a way as to satisfy the molar ratio of 1: 1: 1: 3 according to the calculation of the chemical reaction. The concentrations of Zr, Er, Nd in the initial aliquots were the same (in mole fractions). The onset of equilibrium in the system was established by systematic observation of the sediment height and periodically conducting chemical analysis of control samples of equilibrium solutions. After equilibrium was established, the solid phase was separated from the filtrate, washed several times thoroughly with deionized water and dried in a drying cabinet at a temperature of 50–60 °C.

To determine the composition of the precipitate, qualitative and quantitative elemental analysis of the obtained solid phase was performed using the method of inductively coupled plasma atomic emission spectrometry (ICP-AES) on an iCAP PRO XP device (Thermo Scientific, USA), respectively. To conduct ICP-AES and XRF, tablets were prepared (by pressing the compound under study onto a boric acid substrate); then the samples were transferred into solution under the influence of microwave radiation.

To determine the homogeneity and confirm the composition of the compound, scanning electron (SEM, images were obtained on a Carl Zeiss EVO-10 microscope) and X-ray microanalysis (Energy Dispersive X-ray (EDX) analyses) were performed. The luminescent properties of the obtained substance were determined. Luminescence excitation spectra of powder samples were recorded on a Perkin Elmer LS 55 luminescence spectrometer at room temperature (298 K) in the wavelength range of 300–900 nm, which corresponds to the UV, visible and near IR ranges. A standard holder for solid samples was used for recording; the amount of the studied material did not allow covering the entire area of the holder, which reduced the intensity of the obtained signal.

3. Results and discussion

Equilibrium in the reaction under study was reached after 30–35 days. Starting from the 30th day, the amount of sediment no longer changed. The pH of the filtrate was 2–3, and the temperature was 22 °C.

As a result of the reaction, a greyish-blue precipitate was formed. The precipitate was separated from the filtrate and thoroughly washed several times with deionized water.

Table 1. Results of elemental analysis of the AES-ICP complex (average values based on three determinations; relative standard deviation 1-2%)

Element	Content, wt. %
Na	1.22
Mo	30.98
Zr	7.9
Er	13.62
Nd	7.09

The results of the sample analysis by atomic emission spectroscopy (AES-ICP) are presented in Table 1. Based on the AES-ICP data, it was established that the sample contains all the ions of the initial components.

According to the results of quantitative analysis of ICP-AES, the synthesized solid phase sample is heterogeneous: νNa : νMo : νZr : νEr : νNd = 0.05 : 0.22 : 0.086 : 0.082 : 0.05.

The obtained results of SEM images of the powder sample with different magnifications (in the same area) show some morphological features, such as granularity and a heterogeneous structure (Fig. 1).

The presence of different phases and dispersions have different effects on the formation of physicochemical properties. According to the results of X-ray microanalysis, in 3 selected areas of the sample in the figure, the spectra correspond to overlapping areas. When interpreting the results of elemental analysis, it should be taken into account that the sodium K-line overlaps with the neodymium L-line, and therefore the determination of quantitative ratios may be ambiguous (Fig. 2).

However, when assessing the spatial distribution of the composition, one can notice a close percentage ratio and a certain homogeneity of the solid phase, although it is not expressed very strongly (Table 2).

The resulting compound contains two REE ions (Er and Nd), which emit light in the near IR range (according to the generally accepted concepts of the luminescent properties of REE ions). The Perkin Elmer LS 55 spectrometer allows only partial detection of the luminescence band for the Nd^{3+} ion, corresponding to the 4F3/2-4I9/2 transition in the region of 885 nm (inserted in Fig. 3).

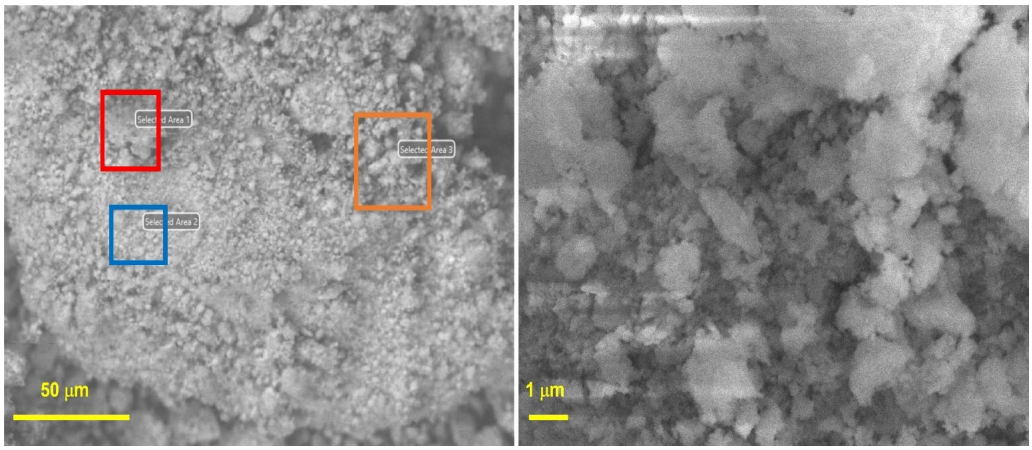

Fig. 1. SEM images of a powder sample.

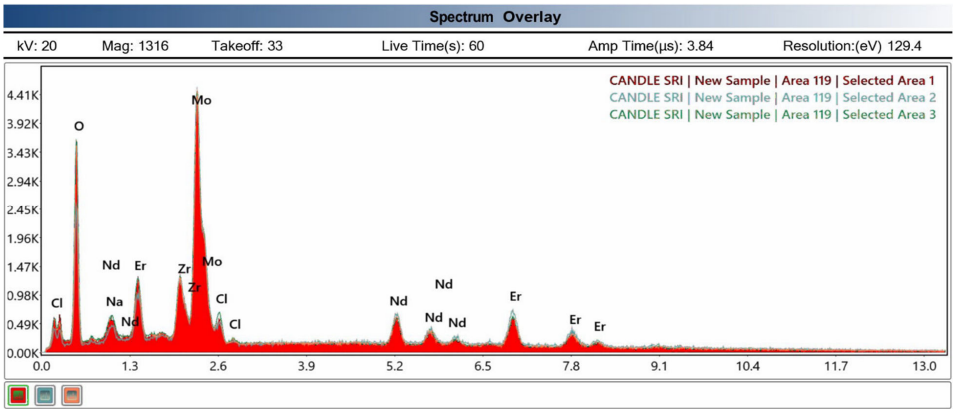

Fig. 2. X-ray microanalysis spectrum of the studied sample.

Table 2. Percentage ratio of elements and assessment of homogeneity of the solid phase.

Element	Weight %	Atomic %	Error %
Zone 119 / Selected Zone 1			
OK	32.42	75.29	10.04
NaK	1.23	1.99	16.15
ZrL	6.6	2.69	6.82
MoL	32.19	12.47	3.64
ClK	1.32	1.38	13.79
NdL	10.34	2.66	7.16
ErL	15.9	3.53	7.84
Zone 119 / Selected Zone 2			
OK	24.1	67.56	10.51
NaK	0.94	1.84	19.1
ZrL	7.39	3.63	7.48
MoL	34.87	16.31	4.12
ClK	1.38	1.74	12.94
NdL	11.99	3.73	8.29
ErL	19.33	5.18	8.03
Zone 119 / Selected Zone 3			
OK	31.68	74.19	10.01
NaK	1.39	2.27	14.29
ZrL	6.34	2.6	7.02
MoL	32.21	12.58	3.6
ClK	1.94	2.06	10.34
NdL	10.73	2.79	7.34
ErL	15.71	3.52	7.66

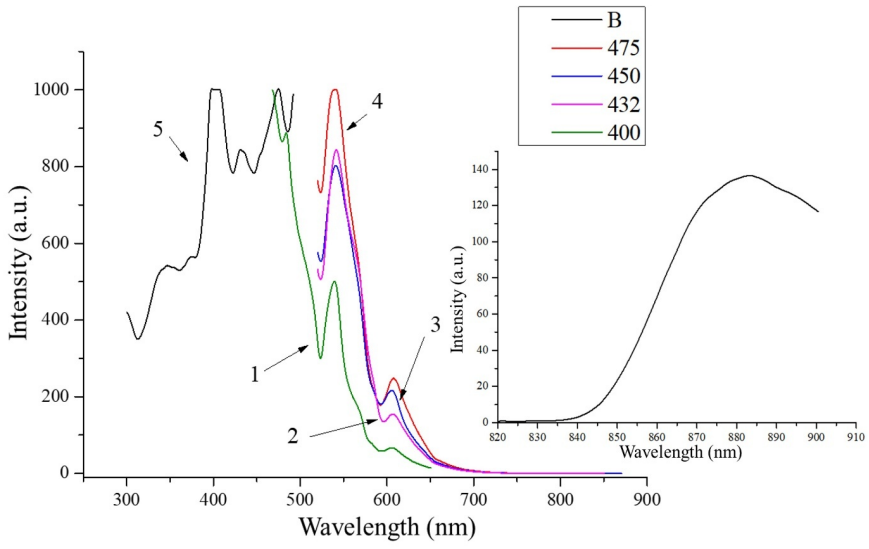

Fig. 3. Luminescence spectra (1-4) recorded at different excitation values, and excitation spectrum (5). 1 – excitation at 400 nm, 2 – excitation at 432 nm, 3 – excitation at 450 nm, 4 – excitation at 475 nm. Excitation spectrum (5) was recorded for the most intense band at 540 nm. Insert – excitation at 400 nm, maximum slit width.

The intensity of this band is weak compared to the intensity of the bands in the visible region of the spectrum, so it was recorded separately, at the maximum slit width of the spectrometer. The erbium photoluminescence band (~1500 nm) cannot be recorded on this spectrometer in principle. It should be noted that the presence of a d-element (Zr) with an unfilled d-shell in the complex apparently causes intense luminescence in the visible region of the spectrum and a complex type of excitation spectrum, although it is known from the literature that the Mo matrix itself exhibits luminescence in the 300–550 nm region under UV excitation.

4. Conclusions

The conducted study demonstrated that a chemical reaction within the investigated system results in the formation of a previously undescribed insoluble solid phase, which represents a novel multicomponent compound incorporating Na, Mo, Zr, Nd, and Er elements originating from the starting reagents. The synthesis of such a heterogeneous material is noteworthy, as it combines multiple rare-earth and transition metal components, providing a promising platform for advanced optical materials development.

Comprehensive elemental analysis confirmed the stoichiometric inclusion of all expected elements, validating the successful incorporation of Nd^{3+} and Er^{3+} ions into the crystal matrix. Detailed morphological characterization revealed a complex, multiphase nanostructure, with clear evidence of nanoscale domains and heterogeneous particle distribution. These structural features may play a significant role in defining the optical and luminescent behavior of the material.

The photophysical investigation of the synthesized phase revealed a characteristic emission band of Nd^{3+} ions at approximately 885 nm, corresponding to the 4F3/2-4I9/2 transition, which was partially resolved under the selected excitation conditions. The observed spectral properties indicate that this compound can be considered a promising candidate for the design of laser-active materials and further functional optical devices.

Thus, the novelty of this work lies not only in the synthesis of a new, insoluble, rare-earth-containing solid phase but also in its detailed structural elucidation and demonstration of practical luminescent potential. Future studies will focus on fine-tuning its synthesis parameters, exploring energy transfer mechanisms between Nd^{3+} and Er^{3+} centers, and evaluating its performance in prototype laser systems.

Acknowledgement

This work was supported by the Higher Education and Science Committee MESCS RA [Research project № 25YR-1D022].

References

[1]. H. Safardoust-Hojaghan, 10 – Rare-earth molybdates ceramic nanomaterials, Advanced Rare Earth-Based Ceramic Nanomaterials (2022) 259–290. DOI: 10.1016/B978-0-323-89957-4.00001-3

[2]. M.R.N. Soares, Development of Zirconia Based Phosphors for Application in Lighting and as Luminescent Bioprobes, Ph.D. Thesis, University of Aveiro, Aveiro, Portugal, 2016.

[3]. V. Balaram, Sources and applications of rare earth elements, in: Environmental Technologies to Treat Rare Earth Elements Pollution: Principles and Engineering, IWA Publishing, London, UK, 2022, pp. 75–113. DOI: 10.2166/9781789062236

[4]. T.S. Berezhnaya, K.A. Chebyshev, R.V. Kabanov, New fluorite-like lanthanum-europium molybdates with $Nd_5Mo_3O_{16+\delta}$-type structure, *J. Alloys Compd.* 1023 (2025) 180138. DOI: 10.1016/j.jallcom.2025.180138

[5]. N.I. Steblevskaya, M.V. Belobeletskaya, M.A. Medkov, Luminescent properties of lanthanum borates $LaBO_3$:Eu and $La(BO_2)_3$:Eu obtained by the extraction-pyrolytic method, *Russ. J. Inorg. Chem*. 66 (2021) 468–476. DOI: 10.1134/S0036023621040215

[6]. A.P. Shablinskii, R.S. Bubnova, I.E. Kolesnikov, et al., Novel $Sr_3Bi_2(BO_3)_4$:Eu^{3+} red phosphor: Synthesis, crystal structure, luminescent and thermal properties, *Solid State Sci.* 70 (2017) 93–100. DOI: 10.1016/j.solidstatesciences.2017.06.009

[7]. I. Gupta, S. Singh, S. Bhagwan, D. Singh, Rare earth (RE) doped phosphors and their emerging applications: A review, *Ceram. Int.* 47 (2021) 19282–19303. DOI: 10.1016/j.ceramint.2021.03.308

[8]. J. Huang, J. Liu, W. Zhao, et al., Synthesis, structure and luminescence properties of a novel red fluorescent material $Ba_2MgB_2O_6$:Eu^{3+}, *Ceram. Int.* 49 (2023) 29607–29613. DOI: 10.1016/j.ceramint.2023.06.177

[9]. K. Singh, M. Rajendran, R. Devi, S. Vaidyanathan, Narrow-band red-emitting phosphors with high color purity, trifling thermal and concentration quenching for hybrid white LEDs and $Li_3Y_3BaSr(MoO_4)_8$:Sm^{3+}, Eu^{3+}-based deep-red LEDs for plant growth applications, *Inorg. Chem.* 61 (2022) 2768–2782. DOI: 10.1021/acs.inorgchem.1c02836

[10]. V. Kalavathi, R.K. Bhuyan, A detailed study on zirconium and its applications in manufacturing process with combinations of other metals, oxides and alloys – A review, *Mater. Today: Proc*. 19 (2019) 781–786. DOI: 10.1016/j.matpr.2019.08.130

[11]. S. Kaushal, V. Kumari, P.P. Singh, Sunlight-driven photocatalytic degradation of ciprofloxacin and organic dyes by biosynthesized rGO-ZrO_2 nanocomposites, *Environ. Sci. Pollut. Res.* 30 (2023) 65602–65617. DOI: 10.1007/s11356-023-27000-6

[12]. Z.Y. Hussien, A.Q. Moften, M.A. Abdulrehman, Review of zirconia (ZrO_2) biomedical applications: Advanced manufacturing techniques and materials properties, *Revue Compos. Mater. Avancés* 35 (2025) 345–353. DOI: 10.18280/rcma.350216

[13]. S. Jakab-Costenoble, I. Rumaux, E. Odore, S. Picart, Synthesis, characterization and solubility of mixed zirconium-cerium molybdate precipitates, *J. Nucl. Sci. Technol.* 55 (2018) 1235–1244. DOI: 10.1080/00223131.2018.1492468

[14]. M. Segundo Sena, M. Medeiros de Santana e Silva, A. Gomes Dos Santos, et al., Synthesis and characterization of cerium molybdate semiconductor nanoparticles, *Mater. Res.* 20 (2017) 485–491. DOI: 10.1590/1980-5373-mr-2017-0092

[15]. S.B. Jaffri, K.S. Ahmad, I. Abrahams, et al., Augmented photovoltaic and electrochemical performance of lanthanide (Ln^{3+} = Ce^{3+}, Pr^{3+}, and Nd^{3+}) doped ZrO_2 semiconductor material, *J. Mater. Sci.: Mater. Electron*. 34 (2023) 1376. DOI: 10.1007/s10854-023-10811-1

[16]. S.R. Sanivarapu, J.B. Lawrence, G. Sreedhar, Role of surface oxygen vacancies and lanthanide contraction phenomenon of $Ln(OH)_3$ (Ln = La, Pr, and Nd) in sulfide-mediated photoelectrochemical water splitting, *ACS Omega* 3 (2018) 6267–6278. DOI: 10.1021/acsomega.8b00429

[17]. A.F. Fuentes, E.C. O'Quinn, S.M. Montemayor, et al., Pyrochlore-type lanthanide titanates and zirconates: Synthesis, structural peculiarities, and properties, *Appl. Phys. Rev.* 11 (2024) 021337. DOI: 10.1063/5.0192415

[18]. S. Lakiza, L. Lopato, Phase diagrams of the systems Al_2O_3-ZrO_2-$Ln(Y)_2O_3$ as a source of multiphase eutectics for creating composite structural and functional materials, *J. Eur. Ceram. Soc.* 31 (2011) 1293–1303. DOI: 10.1016/j.jeurceramsoc.2010.12.004

[19]. L. Yuliantini, M. Djamal, R. Hidayat, et al., Luminescence and Judd-Ofelt analysis of Nd^{3+} ion doped oxyfluoride boro-tellurite glass for near-infrared laser application, *Mater. Today: Proc.* 43 (2021) 2655–2662. DOI: 10.1016/j.matpr.2020.04.631

[20]. A.I. Visan, G.F. Popescu-Pelin, Advanced laser techniques for the development of nature-inspired biomimetic surfaces applied in the medical field, *Coatings* 14 (2024) 1290. DOI: 10.3390/coatings14101290

[21]. S. Tanabe, Glass and rare-earth elements: A personal perspective, *Int. J. Appl. Glass Sci.* 6 (2015) 305–328. DOI: 10.1111/ijag.12142

[22]. C. Pérez-Rodríguez, L.L. Martín, S.F. León-Luis, et al., Relevance of radiative transfer processes on Nd^{3+} doped phosphate glasses for temperature sensing by means of the fluorescence intensity ratio technique, S*ens. Actuators B Chem.* 195 (2014) 324–331. DOI: 10.1016/j.snb.2014.01.037

[23]. Y.H. Kim, N.S.M. Viswanath, S. Unithrattil, et al., Review-Phosphor plates for high-power LED applications: Challenges and opportunities toward perfect lighting, *ECS J. Solid State Sci. Technol*. 7 (2017) R3134. DOI: 10.1149/2.0181801jss

[24]. L.G. Nersisyan, R.S. Arutyunyan, H.R. Petrosyan, Study of reactions in the Na_2MoO_4-$ZrOCl_2$-$ErCl_3$-H_2O system, *Theor. Found. Chem. Eng*. 57 (2023) 108–1087. DOI: 10.1134/S0040579523310068